ChemPubSoc Europe

DOI: 10.1002/ejic.201900067

EurJIC European Journal of Inorganic Chemistry

Full Paper

Tunable Fluorescence

Tuning the Fluorescence Emission and HOMO-LUMO Band Gap in Homoleptic Zinc(II) Complexes with *N*,*O*-Bidentate (Imidazo[1,5-*a*]pyrid-3-yl)phenols

G. Attilio Ardizzoia,[a] Gioele Colombo,[a] Bruno Therrien,[b] and Stefano Brenna*[a]

Abstract: A series of homoleptic zinc(II) complexes of the general formula $[Zn(L^R)_2]$ (HL^R: (imidazo[1,5-*a*]pyrid-3-yl)phenol; R: *para*-substituent to the phenol) have been synthesized. The single-crystal X-ray structure analysis of complex $[Zn(L^H)_2]$ (**1**) confirmed the expected *N*,*O*-bidentate coordination of L^R, via the pyridine-like nitrogen of the imidazo[1,5-*a*]pyridine skeleton and the phenolate oxygen. The photophysical properties of the complexes have been investigated in dichloromethane solution, showing fluorescence emission when excited with UV light (λ_{exc} = 340–360 nm). The intensity and λ_{max} of the emission are both significantly influenced by the R-substituent, the emission maxima moving from blue (R = CF_3, $Zn(L^{CF3})_2$] (**6**)) to orange (R = NO_2, $Zn(L^{NO2})_2$] (**7**). Most of $[Zn(L^R)_2]$ compounds are characterized by moderate-to-good absolute photoluminescence quantum yields, with a maximum of 0.33 for $[Zn(L^H)_2]$ (**1**). Density functional calculations allowed to identify the Natural Transition Orbitals involved in the electronic transitions and define the main transition as being HOMO-LUMO (>95 %) in character. A good linear correlation was found between the HOMO energy and the Hammett σ_p constants associated to the R-substituent, whereas the fluorescence behavior has been described in terms of HOMO-LUMO band gap.

Introduction

The search for efficient systems to be used in optical devices like OLEDs[1] or DSSCs[2] or as fluorescent sensors[3] has led to a relevant expansion of research in organometallic luminescent compounds. Among metal centers, those with d^{10} configuration proved to be a good alternative to the commonly used platinum group metals (PGMs), as documented by publications on optical devices based on coinage metals[4] or zinc and cadmium.[5]

Focusing on the latter, numerous previous works described the significant luminescence behavior of $[M(L)X_2]$ (M = Zn, Cd; X = halide) or $[Zn(L)_n]^{2+}$ compounds, where L indicates a nitrogen bidentate ligand.[6–21] Limited examples have been published with *N*,*O*-ligands, the most relevant being zinc(II) 8-hydroxyquinolinate complexes (Znq_2),[22] which showed highly controllable luminescence properties tuned by substituents on ligand,[23] and high performances in electroluminescent devices.[24] In the latter case, proper substitution of 8-hydroxyquinoline ligands allowed to control the structural and electronic effects which strongly influenced the electroluminescence performances. Low operating voltage OLEDs with the tetrameric $(Znq_2)_4$ compound as emissive layer showed an electroluminescence output about 1.5 times greater than Alq_3 (at 100 μA).[24] Also Schiff base ligands demonstrated to be useful for the synthesis of zinc(II) complexes with remarkable luminescence properties. Very recent examples are fluorescent zinc(II)-salicylaldiminato compounds,[25] dinuclear zinc salphen macrocycle complexes,[26] and zinc(II) and cadmium(II) complexes with piperazino-functionalized *N*,*N*′,*O*-tridentate ligands.[27]

Among nitrogen-based ligands, imidazo-pyridines are known for their interesting photochemical properties, both as free molecules[28–32] and when coordinated to transition metals.[33–38] In our ongoing study on complexes with nitrogen-containing ligands,[39–48] we also investigated zinc(II)[49,50] and silver(I)[51] complexes bearing *N*,*N*-coordinated imidazo-pyridines. Herein, we report on the luminescence properties of a series of homoleptic zinc(II) complexes ($Zn(L^R)_2$) with (imidazo[1,5-*a*]pyrid-3-yl)phenols, which in this case act as *N*,*O*-bidentate ligands. The ligands differ for the substituent R in the *para* position with respect to the hydroxyl group, and the electronic characteristics of R influence in solution the fluorescence of the corresponding complexes. The zinc(II) derivatives $[Zn(L^R)_2]$ show interesting photophysical properties in dichloromethane solution, from λ_{max} of emission tunable by the electronic character of R, to large Stokes shifts and moderate-to-good absolute quantum yields.

Results and Discussion

Synthesis and Characterization

The (imidazo[1,5-*a*]pyrid-3-yl)phenol ligands HL^R (R = H, OMe, Me, F, Br, CF_3, NO_2) were synthesized following an established

[a] *Department of Science and High Technology, University of Insubria and CIRCC, Via Valleggio, 9 – 22100 Como, Italy*
E-mail: stefano.brenna@uninsubria.it
http://www.uninsubria.it/docenti/stefano.brenna
[b] *Institute of Chemistry, University of Neuchâtel, Avenue de Bellevaux 51, CH-2000, Neuchâtel, Switzerland*
Supporting information and ORCID(s) from the author(s) for this article are available on the WWW under https://doi.org/10.1002/ejic.201900067.

procedure[52] by reacting 2-acetylpyridine with two equivalents of 2-hydroxy-5-substituted benzaldehydes in acetic acid, in the presence of ammonium acetate (5 equiv.) as source of the sp^2 nitrogen of the desired heterocycle (Scheme 1). 2-Hydroxy-5-(trifluoromethyl)benzaldehyde[53] is not commercially available and was prepared following literature methods. All (imidazo[1,5-*a*]pyrid-3-yl)phenols were obtained in moderate to good yields and their purity was assessed by ^{1}H NMR, ^{13}C NMR and elemental analysis.

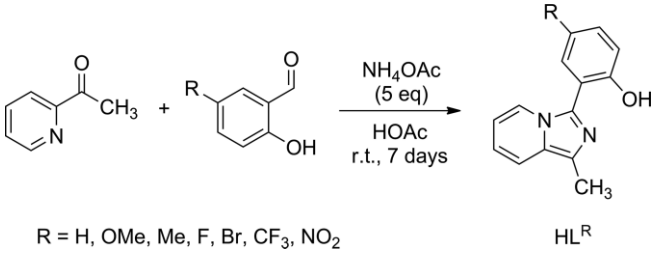

Scheme 1. One-pot synthesis of imidazo[1,5-*a*]pyridin-phenol ligands HL^R from the reaction of 2-acetylpyridine with 2-hydroxy-5-substituted benzaldehydes.

The $[Zn(L^R)_2]$ derivatives were prepared by reacting zinc(II) perchlorate hexahydrate with two equivalents of the corresponding ligand, in acetonitrile, in the presence of a slight excess of triethylamine (Scheme 2). All complexes were obtained as yellow or light brown crystalline powders and they have been first characterized by elemental analysis and infrared spectroscopy. In their infrared spectrum (nujol mull) the $[Zn(L^R)_2]$ compounds show the typical pattern of the ligands, with sharp and intense stretching bands in the region 1515–1620 cm^{-1} ($\upsilon_{C=N}$). The ^{1}H NMR spectra ([D$_6$]DMSO, 25 °C) of complexes **1–7** are reported in Figures S1-S7 (see Supporting Information). They show the expected signals of the corresponding HL^R ligands, with some shifts due to the *N*,*O*-coordination to the metal center. Unfortunately, due to the low solubility of all complexes (with the exception of complex **3**), no information concerning quaternary carbons were obtained from the ^{13}C NMR spectra. Nevertheless, all carbons containing C–H bonds were assigned according to HSQC experiments (Figures S8–S14).

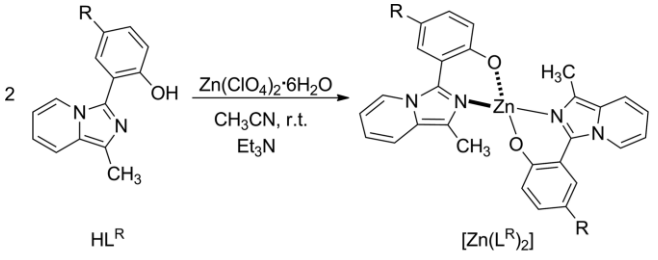

Scheme 2. Synthesis of zinc(II) complexes **1–7**.

Crystal Structure

Most attempts to grow single crystals of complexes **1–7** failed; however, we were successful in the case of compound $[Zn(L^H)_2]$ (**1**), which crystallized in ethanol as the solvate compound **1**·0.5EtOH. As expected, in the crystal structure of **1**, the two L^H ligands are bound in a *N*,*O*-bidentate fashion and the zinc atom possesses a distorted tetrahedral geometry (Figure 1), being coordinated by two nitrogen atoms and two oxygen atoms of two (imidazo[1,5-*a*]pyrid-3-yl)phenol ligands. $[Zn(L^H)_2]$·0.5EtOH shows two independent molecules in the asymmetric unit, one of them being hydrogen-bonded to the ethanol molecule. The O···O distance between the phenolato oxygen and the oxygen of the hydroxyl group of ethanol is 2.786(9). This O···H–O interaction creates differences in the bond lengths around the Zn atom (Table 1). The phenolato oxygen involved in the hydrogen-bond has the longest Zn–O distance at 1.362(10) Å.

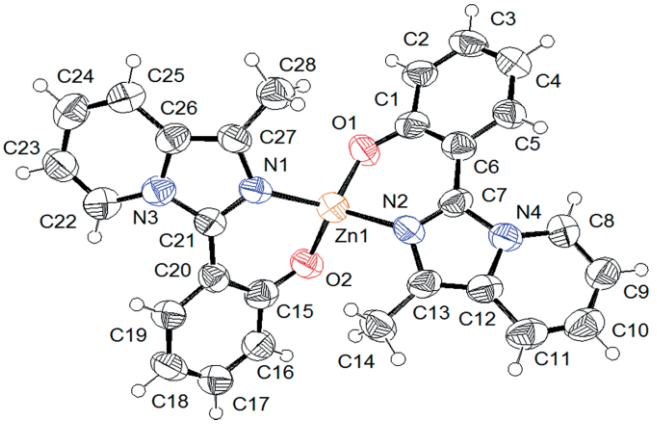

Figure 1. ORTEP representation of one molecule of $[Zn(L^H)_2]$ at 50 % probability level ellipsoids.

Table 1. Selected bond lengths [Å] and angles [°] for the two independent molecules of $[Zn(L^H)_2]$ in the crystal packing of **1**·0.5EtOH.

	Molecule 1		Molecule 2	
Zn–O	1.905(6)	1.902(7)	1.928(6)	1.916(6)
Zn–N	1.983(8)	1.998(7)	1.991(6)	1.966(8)
C-$O_{phenolate}$	1.308(11)	1.336(11)	1.362(10)	1.317(11)
N-Zn–N	127.4(3)		114.7(3)	
O-Zn–O	113.7(3)		116.1(3)	
O-Zn–N	113.3(3)	109.1(3)	118.6(3)	118.1(3)
O-Zn–N	96.6(3)	97.4(3)	95.6(3)	95.4(3)

In both molecules, the zinc atoms show a slightly distorted tetrahedral geometry (Table 1). The calculated τ_4 values[54] are 0.843 (Zn1) and 0.874 (Zn2), respectively. The ligands are not planar, the phenolic rings rotate along the C–C bond and the plane containing the imidazo-pyridine skeleton and the phenol plane are twisted by about 35–39°.

Optical Properties in Solution

The photophysical data for all compounds are collected in Table 2. Figure 2 reports the normalized UV/Vis, excitation and emission spectra recorded in dichloromethane solution (5×10^{-5} M) for complex $[Zn(L^H)_2]$ (**1**), taken as a representative example of the series. The normalized UV/Vis, excitation and emission spectra of all complexes are reported in Figure S15 (Supporting Information).

Table 2. Photophysical data for the zinc(II) complexes **1–7** recorded in solution (CH_2Cl_2, 5×10^{-5} M).

	R	λ_{abs} [nm]	ε (M^{-1} cm^{-1})	λ_{exc} [nm]	λ_{em} [nm]	Stokes shift [nm]	[eV]	Φ_{PL}	τ [ns]
1	H	340	35020	356	490	134	0.95	0.33	2.8
2	OMe	360	26660	385	527	142	0.87	0.10	2.2
3	Me	354	30340	353	496	143	1.01	0.22	2.7
4	F	349	31120	367	491	124	0.85	0.23	3.1
5	Br	362	23060	367	484	117	0.82	0.13	2.4
6	CF_3	350	30900	350	473	123	0.92	0.21	2.8
7	NO_2	350	27560	397	615	218	1.11	<0.05	–

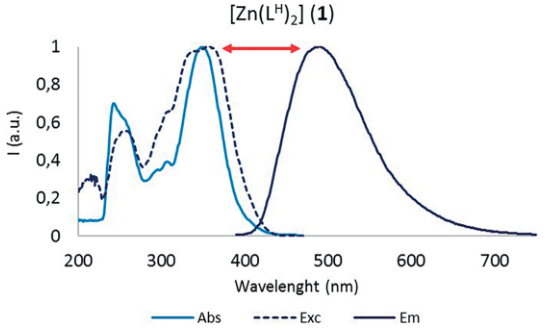

Figure 2. Normalized UV/Vis (light blue), excitation (dashed) and emission (solid blue) spectra of complex $[Zn(L^H)_2]$, **1** (CH_2Cl_2, 5×10^{-5} M). The red arrow highlights the high Stokes shift observed.

The red arrow in Figure 2 highlights the high Stokes shift (117–218 nm, 0.82–1.11 eV) which characterizes all these complexes, with a very low superposition of excitation and emission profiles. All the compounds in the series show quite similar UV/Vis traces, characterized by two main absorption peaks respectively at about 240–260 nm and in the wavelength range between 340 nm and 360 nm (Table 2). These features resemble those of the UV/Vis spectra of free ligands in dichloromethane solution (Figure S16).

Both these characteristics (i.e., high Stokes shift and similar UV/Vis spectra compared to ligands) gave us confidence about the possibility to transfer the photophysical properties of our (imidazo[1,5-*a*]pyrid-3-yl)phenol ligands HL^R to the corresponding zinc(II) complexes, with an enhancement of efficiency due to the coordination to zinc(II). Thus, a possible influence of the electronic character of substituent R of the ligand on the photophysical behavior of the zinc(II) complexes could be expected. Indeed, the emission spectra of complexes **1–7** (CH_2Cl_2, 5×10^{-5} M) confirmed this hypothesis. They are shown all together in Figure 3, which shows that the electronic character of R influences both the intensity and the energy (i.e., λ_{max}) of the emission (ranging from 456 nm for $[Zn(L^{CF3})_2]$ (**6**) to 615 nm for $[Zn(L^{NO2})_2]$ (**7**)).

All the complexes are characterized by a fluorescence behavior with lifetime decay of few nanoseconds, with the exception of complex $[Zn(L^{NO2})_2]$ (**7**) for which it was not possible to measure a lifetime decay due to very poor emissive response when excited with the pulsed source (320 nm). Compounds **1–6** show a mono-exponential fit of the decay curve (Figure S17), with lifetimes in the range 2.2–3.1 ns. The fluorescence lifetimes of complexes **1–6** are in accord with those of free ligands HL^R

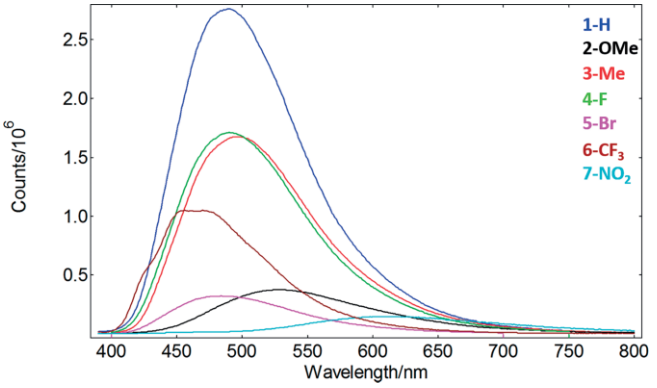

Figure 3. Emission spectra for complexes $[Zn(L^R)_2]$ **1–7**, recorded in solution (CH_2Cl_2, 5×10^{-5} M).

(Table S1), hence reasonably the zinc(II) atom does not take part in the electronic transitions involved in emissive processes (vide infra). The metal center plays a structural role in these complexes, avoiding any possible rotational mode and consequently giving rigidity to the whole system. This is somehow corroborated by the absolute quantum yields (Φ_{PL}) measured in solution (Table 2): indeed, complexes **1** (R = H), **3** (R = Me), **4** (R = F), **5** (R = Br) and **6** (R = CF_3) are characterized by good Φ_{PL} values (the highest being recorded for compound $[Zn(L^H)_2]$ (**1**) (Φ_{PL} = 0.33)), which are always greater than the Φ_{PL} values recorded for the corresponding free ligands HL^R (Table S1). Complex **2** (R = OMe) is characterized by a quite poor quantum yield, whereas complex **7** (R = NO_2) shows no emission in solution, as a consequence of the introduction of the nitro substituent, which is known to act as a fluorescence quencher.[23]

DFT Calculations

To get better insights on the nature of the transitions responsible for the absorption and emission processes, TD-DFT calculations were performed on complexes **1–7**. First, starting from the X-ray crystal structure of complex **1**, the geometries of the complexes were fully optimized at the DFT/PBE-D3 level of theory. The optimized geometries of compounds **1–7** are in good agreement with the available X-ray data (see Supporting Information for the coordinates of the optimized structures). Then, the frontier molecular orbitals and the UV/Vis spectra for complexes **1–7** have been calculated. The calculated vs. experimental UV/Vis spectra in solution for compound $[Zn(L^H)_2]$ (**1**), again taken as a representative example, are reported in Figure 4, whereas HOMO and LUMO orbitals for all compounds are depicted in Figure 5. Table 3 reports the energies of HOMO and LUMO orbitals.

The shape of the frontier orbitals is quite similar for all the zinc(II) derivatives: the HOMO is distributed over both the imidazo-pyridine and the phenolic portion of the molecule, while the LUMO is nearly entirely localized on the imidazo-pyridine skeleton, which is known to usually act as the acceptor portion. The only exception is represented by the LUMO orbital of complex $[Zn(L^{NO2})_2]$ (**7**), which is totally localized on the phenolic moiety and shows no contribution from the imidazo-pyridine

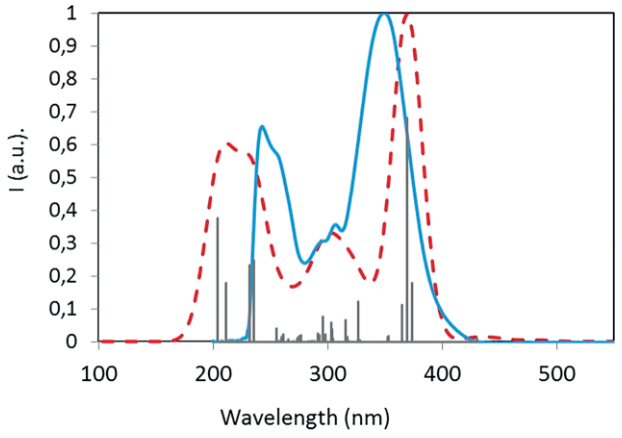

Figure 4. Calculated (dotted blue) vs. experimental (red) UV/Vis spectra of complex $[Zn(L^{H})_2]$ (**1**).

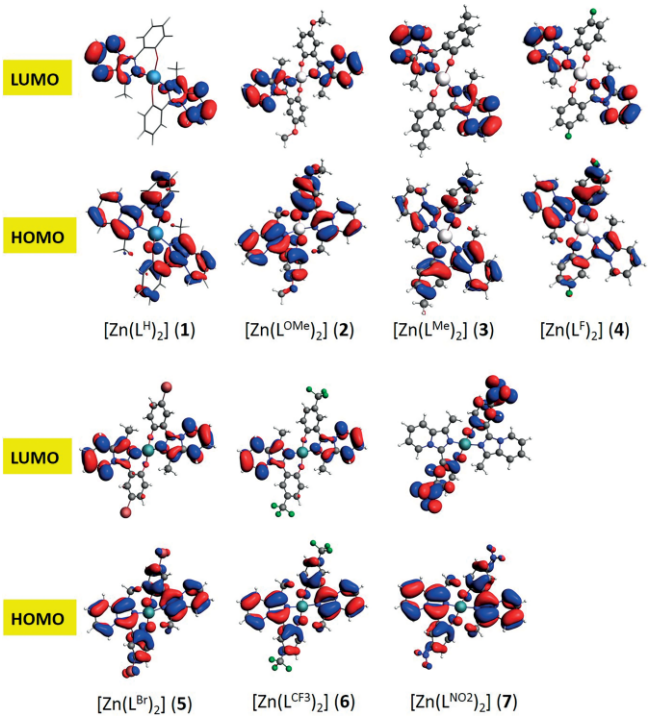

Figure 5. Frontier molecular orbitals for the zinc(II) derivatives **1–7**.

Table 3. HOMO/LUMO energies for zinc(II) complexes **1–7**; last column: Hammett σ_p constants for substituents R.[55]

$[Zn(L^{R})_2]$	R	E_{HOMO} [eV]	E_{LUMO} [eV]	H-L gap [eV]	σ_p
1	H	–5.580	–1.353	4.227	0
2	OMe	–5.403	–1.371	4.032	–0.27
3	Me	–5.489	–1.395	4.194	–0.17
4	F	–5.616	–1.395	4.221	0.06
5	Br	–5.647	–1.422	4.225	0.23
6	CF_3	–5.766	–1.442	4.324	0.54
7	NO_2	–5.902	–2.467	3.435	0.78

skeleton (Figure 5). This is also reflected by the shapes of the corresponding Natural Transition Orbitals (NTOs) calculated for the complexes (Figure 6). Indeed, the absorption at lower energy has been defined nearly as a HOMO-LUMO transition for all species, thus for complexes **1–6** the donor orbital is distributed both on the imidazo-pyridine and the phenolic moieties, while the virtual (acceptor) orbital is localized on the imidazo-pyridine part. Differently, the acceptor orbital for compound $[Zn(L^{NO2})_2]$ (**7**), reminiscent of the LUMO shape, does not comprise the imidazo-pyridine moiety and is confined only on the phenolic residue.

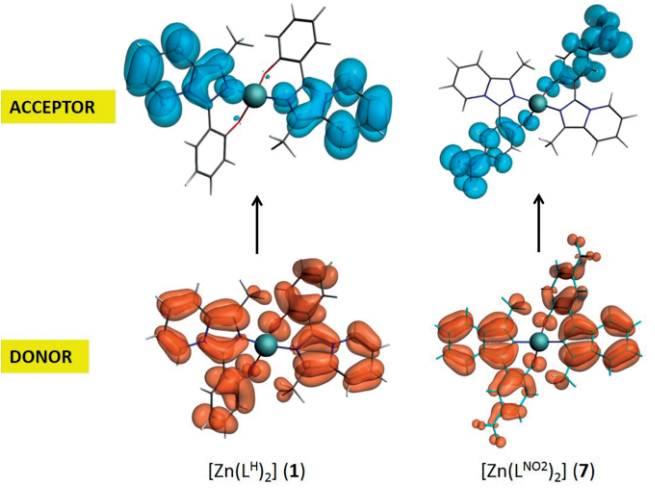

Figure 6. Dominant natural transition orbitals (NTO) pair of the principal (>95 %) electronic transition $S_0 \rightarrow S_1$ in complexes $[Zn(L^{H})_2]$ (**1**) and $[Zn(L^{NO2})_2]$ (**7**).

As said (Figure 3), the electronic character of substituent R influences both the intensity and λ_{max} of the emission. Thus, is reasonably foreseeable the existence of a correlation between the calculated energy of frontier orbitals involved in the electronic transition associated to emission, and the donor/acceptor character of R. The latter can actually be described by the Hammett σ_p constant[55] of R (Table 3).

First, we focused on the energies of HOMOs, which are the frontier orbitals with a tangible contribution from the phenolic residue (and thus from substituent R). A good linear correlation between the σ_p constants and the energy of HOMO orbital for all the zinc(II) complexes could be found (Figure 7, top), the E_{HOMO} increasing with decreasing σ_p (i.e., with increasing donor strength of the substituent). As a result, the energy of the HOMO orbital can be modulated according to the electronic character of substituent R *para* to the hydroxyl group.

Furthermore, we noticed that substituents as H, F and Br, which are quite dissimilar in nature and possess different σ_p constants (σ_p = 0 (H), 0.06 (F), 0.23 (Br), Table 3) led to zinc(II) complexes with a very close emission (λ_{em} = 490 nm (H), 491 (F), 484 (Br), Table 3). This could be explained by considering the HOMO-LUMO energy gap: actually, a linear correlation can be noticed between λ_{em} and the HOMO-LUMO energy gap for all $[Zn(L^{R})_2]$ complexes. Thus, since the zinc(II) complexes having those substituents (H, F, Br) are characterized by very close HOMO-LUMO energy gaps (4.227 (H), 4.221 (F), 4.225 (Br) eV, Table 3), one could expect that their emission is also very similar (Figure 7, bottom). It can thus be concluded that substituent R influences the HOMO energy, and consequently the HOMO-

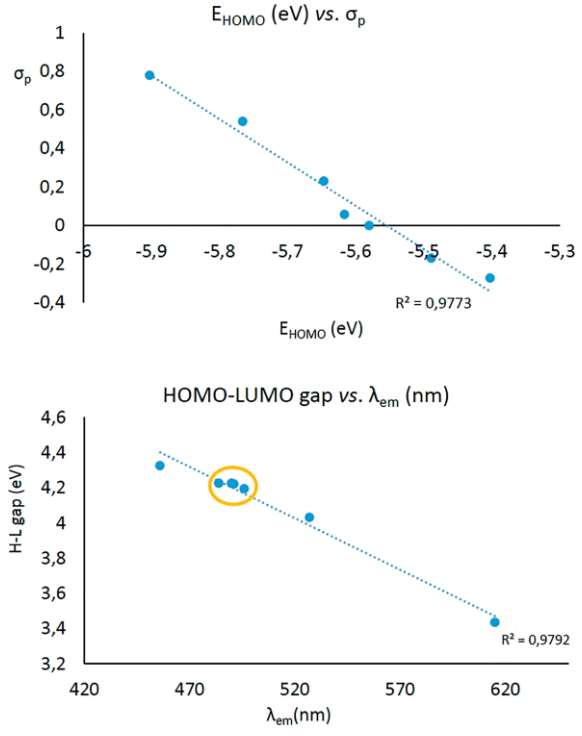

Figure 7. Top: linear correlation between the energy of the HOMO orbital (eV) in zinc(II) complexes **1–7** and the σ_p constants of the corresponding substituents R. Bottom: linear correlation between λ_{em} and the HOMO-LUMO energy gap in complexes **1–7**. The yellow circle highlights facts associated to H, F and Br substituents.

LUMO energy gap, ultimately leading to a tunable emission according to the electronic properties of the ligand.

Conclusions

In this work, we presented the synthesis of a series of homoleptic zinc(II) complexes with *N*,*O*-bidentate (imidazo[1,5-*a*]pyridin-3-yl)phenol ligands, having different substituent R in the *para* position of the hydroxyl group. The single-crystal X-ray structure analysis of **1**·0.5EtOH shows the zinc(II) center in the expected tetrahedral geometry, with a N_2O_2 environment. As a result, the zinc atom plays a structural role which appears to be crucial in the photophysical properties. Indeed, the remarkable characteristics of the (imidazo[1,5-*a*]pyridine)-based ligands (i.e.: high Stokes shift, good quantum yields, high tunability) have been transferred from the ligands to the complexes. In particular, we observed an increase in absolute quantum yields on going from free ligands to the metal complexes, together with high Stokes shift (> 117 nm) and a fluorescence emission that is highly modulated by the electronic character of the substituent R (expressed in term of Hammett constants). TD-DFT calculations were used to elucidate the optical behavior in solution for these compounds and to establish a relation between the emission maxima and the HOMO-LUMO energy gap calculated for the complexes.

Experimental Section

General Remarks: Caution! Although we have experienced no difficulties, perchlorate salts of metal complexes in the presence of organic ligands are potentially explosive and should be handled with care even in small quantities. Despite being not strictly necessary, all syntheses were carried out under argon using standard Schlenk techniques. NMR spectra were recorded with an AVANCE 400 Bruker spectrometer at 400 MHz for ^{1}H NMR and 100 MHz for ^{13}C{^{1}H} NMR. Chemical shifts are given as δ values in ppm relative to residual solvent peaks as the internal reference. ^{13}C NMR spectra were ^{1}H-decoupled and the determination of the multiplicities was achieved by the APT pulse sequence. Elemental analyses were obtained with a Perkin-Elmer CHN Analyzer 2400 Series II. Infrared Spectra were acquired on a Shimadzu Prestige-21 spectrophotometer with a 1 cm^{-1} resolution. The UV/Vis, excitation and emission spectra were measured using a fluorescence spectrophotometer (Edinburgh Instrument FS5) equipped with a 150 W continuous Xenon lamp as a light source and were corrected for the wavelength response of the instrument; lifetime measurements were performed on the same FS5 Edinburgh Instruments equipped with a EPLED-320 (320 nm, Edinburgh Instruments) as the pulsed source. Analysis of the lifetime decay curve was performed using Fluoracle® Software package (Ver. 1.9.1) which runs the FS5 Edinburgh Instrument. Absolute fluorescence quantum yields were determined using a PhotoMed GmbH K-Sphere Integrating Sphere (3.2 inch. diameter). 2-Hydroxy-5-(trifluoromethyl)benzaldehyde[53] was prepared following literature methods; all other chemicals were of reagent grade quality, were purchased commercially (AlfaAesar, Acros, TCI Chemicals) and used as received.

Synthesis of (Imidazo[1,5-*a*]pyrid-3-yl)phenol Ligands HL^R

A mixture of 2-acetylpyridine (2 mL, 17.8 mmol, 1 equiv.), 2-hydroxy-5-substituted benzaldehyde (35.7 mmol, 2 equiv.) and ammonium acetate (6.87 g, 89.2 mmol, 5 equiv.) in deoxygenated glacial acetic acid (40 mL) was stirred at room temperature for 7 days. Then the mixture was poured into 150 mL of water and extracted with CH_2Cl_2 (3 × 70 mL). The organic phase was washed with a saturated aqueous solution of $NaHCO_3$, dried with Na_2SO_4 and the suspension was filtered. The solvent was evaporated under vacuum, and the crude product was recrystallized with hexane or diethyl ether.

In the case of R = Me, F and Br, the precipitation of a small quantity of a red solid occurred. This was filtered off, washed with water and methanol, then dried. ^{1}H and ^{13}C NMR analysis ($CDCl_3$, 25 °C) allowed to identify it as 8*H*,16*H*-8,16-epiminodinaphtho[2,1-*b*:2′,1′-*f*][1,5]dioxocine.[56] After removal of the red solid, the filtrate was poured into water (150 mL) and extracted with CH_2Cl_2 (3 × 70 mL). The organic phase was washed with a saturated aqueous solution of $NaHCO_3$, dried with Na_2SO_4 and the suspension was filtered. The solvent was evaporated under vacuum, and the crude product was recrystallized with hexane or diethyl ether.

In the case of R = NO_2, the product precipitated from the bulk as an orange solid. After seven days, it was filtered and washed with acetic acid and with abundant water.

General Procedure for the Synthesis of Complexes [Zn(L^R)$_2$] 1–7

Zinc(II) perchlorate hexaydrate (0.15 g, 0.403 mmol) was dissolved in deoxygenated acetonitrile (10 mL) and two equivalents (0.806 mmol) of ligand HL^R were added. The mixture was stirred at room temperature for 15 minutes, then Et_3N (200 µL, 1.44 mmol) was added and the suspension further stirred for 12 h. Then the yellow-to-brown solid was filtered off, washed with water, acetonitrile and diethyl ether, and dried under vacuum.

$[Zn(L^{H})_2]$ (1): Yield 0.153 g (74 %). Elemental analysis (%) calcd. for $C_{28}H_{22}N_4O_2Zn$: C 65.70, H 4.33, N 10.95. Found C 65.60, H 4.48, N 10.74 %. ^{1}H NMR (400 MHz, [D$_6$]DMSO, 25 °C): δ = 2.12 (s, 3H), 6.69 (d, $^3J_{H,H}$ = 7.8 Hz, 1H), 6.85 (m, 3H), 7.20 (t, $^3J_{H,H}$ = 7.9 Hz, 1H), 7.65 (t, $^3J_{H,H}$ = 7.1 Hz, 2H), 8.56 (d, $^3J_{H,H}$ = 7.4 Hz, 1H). ^{13}C NMR (100 MHz, [D$_6$]DMSO, 25 °C): δ = 11.01 (CH$_3$), 114.22 (Ar-C), 115.66 (Ar-C), 118.76 (Ar-C), 119.92 (Ar-C), 122.86 (Ar-C), 123.21 (Ar-C), 127.06 (Ar-C), 131.34 (Ar-C). X-ray quality crystals were grown by slow diffusion of diethyl ether into a solution of **1** in ethanol.

$[Zn(L^{OMe})_2]$ (2): Yield 0.157 g (68 %). Elemental analysis (%) calcd. for $C_{30}H_{26}N_4O_4Zn$: C 63.00, H 4.58, N 9.80. Found C 62.80, H 4.67, N 9.55 %. ^{1}H NMR (400 MHz, [D$_6$]DMSO, 25 °C): δ = 2.11 (s, 3H), 3.75 (s, 3H), 6.78 (d, $^3J_{H,H}$ = 9.0 Hz, 1H), 6.88 (m, 3H), 7.16 (d, $^3J_{H,H}$ = 3.1 Hz, 1H), 7.66 (d, $^3J_{H,H}$ = 8.9 Hz, 1H), 8.64 (d, $^3J_{H,H}$ = 7.3 Hz, 1H).

$[Zn(L^{Me})_2]$ (3): Yield 0.126 g (58 %). Elemental analysis (%) calcd. for $C_{30}H_{26}N_4O_2Zn$: C 66.73, H 4.85, N 10.38. Found C 66.49, H 4.80, N 10.26 %. ^{1}H NMR (400 MHz, [D$_6$]DMSO, 25 °C): δ = 2.10 (s, 3H), 2.27 (s, 3H), 6.75 (d, $^3J_{H,H}$ = 8.3 Hz, 1H), 6.84 (dt, $^3J_{H,H}$ = 17.6, 6.6 Hz, 2H), 7.01 (d, $^3J_{H,H}$ = 8.4 Hz, 1H), 7.43 (s, 1H), 7.62 (d, $^3J_{H,H}$ = 8.9 Hz, 1H), 8.59 (d, $^3J_{H,H}$ = 7.3 Hz, 1H). ^{13}C NMR (100 MHz, [D$_6$]DMSO, 25 °C): δ = 10.81 (CH$_3$), 20.16 (CH$_3$), 112.34 (C$_q$), 115.01 (Ar-C), 118.43 (Ar-C), 119.56 (Ar-C), 121.89 (C$_q$), 122.11 (Ar-C), 122.83 (Ar-C), 124.94 (C$_q$), 126.23 (Ar-C), 126.31 (C$_q$), 131.84 (Ar-C), 136.45 (C$_q$), 163.81 (C$_q$).

$[Zn(L^{F})_2]$ (4): Yield 0.124 g (56 %). Elemental analysis (%) calcd. for $C_{28}H_{20}F_2N_4O_2Zn$: C 61.38, H 3.68, N 10.23. Found C 61.60, H 3.52, N 10.11 %. ^{1}H NMR (400 MHz, [D$_6$]DMSO, 25 °C): δ = 2.14 (s, 3H), 6.87 (m, 3H), 7.05 (s, 1H), 7.46 (d, $^3J_{H,H}$ = 8.9 Hz, 1H), 7.66 (d, $^3J_{H,H}$ = 8.9 Hz, 1H), 8.60 (s, 1H).

$[Zn(L^{Br})_2]$ (5): Yield 0.132 g (47 %). Elemental analysis (%) calcd. for $C_{28}H_{20}Br_2N_4O_2Zn$: C 50.22, H 3.01, N 8.37. Found C 50.45, H 3.12, N 8.60 %. ^{1}H NMR (400 MHz, [D$_6$]DMSO, 25 °C): δ = 2.18 (s, 3H), 6.83 (m, 3H), 7.29 (s, 1H), 7.59–7.85 (m, 2H), 8.50 (s, 1H).

$[Zn(L^{CF3})_2]$ (6): Yield 0.177 g (68 %). Elemental analysis (%) calcd. for $C_{30}H_{20}F_6N_4O_2Zn$: C 55.62, H 3.11, N 8.65. Found C 55.33, H 3.18, N 8.91 %. ^{1}H NMR (400 MHz, [D$_6$]DMSO, 25 °C): δ = 2.23 (s, 3H), 6.82–7.14 (m, 3H), 7.37–7.63 (m, 1H), 7.70 (d, $^3J_{H,H}$ = 9.0 Hz, 1H), 7.94 (s, 1H), 8.39–8.57 (m, 1H).

$[Zn(L^{NO2})_2]$ (7): Yield 0.145 g (60 %). Elemental analysis (%) calcd. for $C_{28}H_{20}N_6O_6Zn$: C 55.88, H 3.35, N 13.96. Found C 55.56, H 3.21, N 13.82 %. ^{1}H NMR (400 MHz, [D$_6$]DMSO, 25 °C): δ = 2.41 (s, 3H), 6.76 (d, $^3J_{H,H}$ = 9.3 Hz, 1H), 6.88 (dt, $^3J_{H,H}$ = 17.4, 6.6 Hz, 2H), 7.71 (d, $^3J_{H,H}$ = 8.9 Hz, 1H), 8.04 (dd, $^3J_{H,H}$ = 9.3, 3.0 Hz, 1H), 8.53 (t, $^3J_{H,H}$ = 6.5 Hz, 2H).

X-ray Crystallography

A crystal of complex **1**·0.5EtOH was mounted on a Stoe Image Plate Diffraction system equipped with a ϕ circle goniometer, using Mo-K_α graphite monochromated radiation (λ = 0.71073 Å) with ϕ range 0–200°. The structure was solved by direct methods using the program SHELXS–97, while refinement and all further calculations were carried out using SHELXL–97.[57] The H-atoms were included in calculated positions and treated as riding atoms using the SHELXL default parameters. The non-H atoms were refined anisotropically, using weighted full-matrix least-square on F^2. Crystallographic details are summarized in Table S2. Figure 1 was drawn with ORTEP–32.[58]

CCDC 1890067 (for **1**·0.5EtOH) contains the supplementary crystallographic data for this paper. These data can be obtained free of charge from The Cambridge Crystallographic Data Centre.

Computational Details

All calculations were carried out at the density functional (DFT) level of theory with the ADF2017.113 program package.[59] The PBE functional plus a D3 dispersion correction energy term (PBE-D3)[60] was employed for all calculations. Frequency analysis were performed for all optimized structures to establish the nature of the stationary points. TD-DFT implemented in the ADF package was used to determine the excitation energies: the 40 lowest singlet-singlet excitations were calculated by using the optimized geometries. For geometry optimizations, the C, H, N, O and F atoms were described through TZ2P basis sets [triple-ξ Slater-type orbitals (STOs) plus two polarization function]; QZ4P basis set (quadruple-ζ STO plus four polarization functions) was used for Zn and Br atoms. The corresponding augmented basis set was employed in TD-DFT calculations.[61] Restricted formalism, no-frozen-core approximation (all-electron) and no-symmetry constrains were used in all calculations. Solvent effects (CH_2Cl_2) were simulated employing the conductor-like continuum solvent model (COSMO)[62] as implemented in the ADF suite.

Acknowledgments

S. B. and G. A. A. thank the Ministero dell'Università e della Ricerca (MIUR) and the University of Insubria (grant CSR-12) for financial support. Fondazione Banca del Monte di Lombardia (FBML) is also greatly acknowledged for generous funding through the Research Project "*Transiton-metals based coordination compounds for light emitting device applications*".

Keywords: Fluorescence · N ligands · Density functional calculations · Zinc · Photochemistry

[1] G. M. Farinola, R. Ragni, *Chem. Soc. Rev.* **2011**, *40*, 3467–3482.
[2] M. Grätzel, *Acc. Chem. Res.* **2009**, *42*, 1788–1798.
[3] M. L. Aulsebrook, B. Graham, M. R. Grace, K. L. Tuck, *Coord. Chem. Rev.* **2018**, *375*, 191–120, and references cited therein.
[4] C.-W. Hsu, C.-C. Lin, M.-W. Chung, Y. Chi, G.-H. Lee, P.-T. Chou, C.-H. Chang, P.-Y. Chen, *J. Am. Chem. Soc.* **2011**, *133*, 12085–12099.
[5] R. C. Evans, P. Douglas, C. J. Winscom, *Coord. Chem. Rev.* **2006**, *250*, 2093–2126.
[6] Q.-D. Liu, R. Wang, S. Wang, *Dalton Trans.* **2004**, 2073–2079.
[7] C. Seward, J. Pang, S. Wang, *Eur. J. Inorg. Chem.* **2002**, 1390–1399.
[8] R. Tan, Z.-B. Wang, Y. Li, D. J. Kozera, Z.-H. Lu, D. Song, *Inorg. Chem.* **2012**, *51*, 7039–7049.
[9] A. Beitat, S. P. Foxon, C.-C. Brombach, H. Hausmann, F. W. Heinemann, F. Hampel, U. Monkowius, C. Hirtenlehner, G. Knör, S. Schindler, *Dalton Trans.* **2011**, *40*, 5090–5101.
[10] A. S. Roy, P. Saha, P. Mitra, S. S. Maity, S. Ghosh, P. Ghosh, *Dalton Trans.* **2011**, *40*, 7375–7384.
[11] S. V. Larionov, T. E. Kokina, V. F. Plyusnin, L. A. Glinskaya, A. V. Tkachev, Y. A. Bryleva, N. V. Kuratieva, M. I. Rakhmanova, E. S. Vasilyev, *Polyhedron* **2014**, *77*, 75–80.
[12] Y.-W. Dong, R.-Q. Fan, W. Chen, H.-J. Zhang, Y. Song, X. Du, P. Wang, L.-G. Wei, Y.-L. Yang, *Dalton Trans.* **2017**, *46*, 1266–1276.
[13] Y.-W. Dong, R.-Q. Fan, P. Wang, L.-G. Wei, X.-M. Wang, S. Gao, H.-J. Zhang, Y.-L. Yang, Y.-L. Wang, *Inorg. Chem.* **2015**, *54*, 7742–7752.
[14] a) S. Ikeda, S. Kimachi, T. Azumi, *J. Phys. Chem.* **1996**, *100*, 10528–10530; b) S. Ikeda, S. Yamamoto, T. Azumi, G. A. Crosby, *J. Phys. Chem.* **1992**, *96*, 6593–6597.
[15] K. Sénéchal, O. Maury, H. Le Bozec, I. Ledoux, J. Zyss, *J. Am. Chem. Soc.* **2002**, *124*, 4560–4561.
[16] S.-M. Yue, H.-B. Xu, J.-F. Ma, Z.-M. Su, Y.-H. Kan, H.-J. Zhang, *Polyhedron* **2006**, *25*, 635–644.
[17] B. Bozic-Weber, E. C. Constable, N. Hostettler, C. E. Housecroft, R. Schmitt, E. Schönhofer, *Chem. Commun.* **2012**, *48*, 5727–5729.

[18] T. Tsukamoto, R. Aoki, R. Sakamoto, R. Toyoda, M. Shimada, Y. Hattori, M. Asaoka, Y. Kitagawa, E. Nishibori, M. Nakano, H. Nishihara, *Chem. Commun.* **2017**, *53*, 3657–3660.
[19] Y. Ma, S. Liu, H. Yang, Y. Zeng, P. She, N. Zhu, C.-L. Ho, Q. Zhao, W. Huang, W.-Y. Wong, *Inorg. Chem.* **2017**, *56*, 2409–2416.
[20] M. Tsuchiya, R. Sakamoto, M. Shimada, Y. Yamanoi, Y. Hattori, K. Sugimoto, E. Nishibori, H. Nishihara, *Inorg. Chem.* **2016**, *55*, 5732–5734.
[21] X.-M. Wang, S. Chen, R.-Q. Fan, F.-Q. Zhang, Y.-L. Yang, *Dalton Trans.* **2015**, *44*, 8107–8125.
[22] T. Tsuboi, Y. Nakai, Y. Torii, *Cent. Eur. J. Phys.* **2012**, *10*, 524–528.
[23] G. Yuan, Y. Huo, X. Nie, H. Jiang, B. Liu, X. Fang, F. Zhao, *Dalton Trans.* **2013**, *42*, 2921–2929.
[24] L. S. Sapochak, F. E. Benincasa, R. S. Schofield, J. L. Baker, K. K. C. Riccio, D. Fogarty, H. Kohlmann, K. F. Ferris, P. E. Burrows, *J. Am. Chem. Soc.* **2002**, *124*, 6119–6125.
[25] P. Minei, E. Fanizza, A. M. Rodriguez, A. B. Muñoz-García, P. Cimino, M. Pavone, A. Pucci, *RSC Adv.* **2016**, *6*, 17474–17482.
[26] J. A. Marafie, D. D. C. Bradley, C. K. Williams, *Inorg. Chem.* **2017**, *56*, 5688–5695.
[27] I. Majumder, P. Chakraborty, S. Dasgupta, C. Massera, D. Escudero, D. Das, *Inorg. Chem.* **2017**, *56*, 12983–12901.
[28] H. Wang, W. Xu, Z. Wang, L. Yu, K. Xu, *J. Org. Chem.* **2015**, *80*, 2431–2435.
[29] E. Yamaguchi, F. Shibahara, T. Murai, *Chem. Lett.* **2011**, *40*, 939–940.
[30] F. Shibahara, R. Sugiura, E. Yamaguchi, A. Kitagawa, T. Murai, *J. Org. Chem.* **2009**, *74*, 3566–3568.
[31] F. Shibahara, E. Yamaguchi, A. Kitagawa, A. Imai, T. Murai, *Tetrahedron* **2009**, *65*, 5062–5073.
[32] S. A. Siddiqui, T. M. Potewar, R. J. Lahoti, K. V. Srinivasan, *Synthesis* **2006**, *17*, 2849–2854.
[33] L. Salassa, A. Albertino, C. Garino, G. Volpi, C. Nervi, R. Gobetto, K. I. Hardcastle, *Organometallics* **2008**, *27*, 1427–1435.
[34] C. Garino, T. Ruiu, L. Salassa, A. Albertino, G. Volpi, C. Nervi, R. Gobetto, K. I. Hardcastle, *Eur. J. Inorg. Chem.* **2008**, 3587–3591.
[35] M. D. Weber, C. Garino, G. Volpi, E. Casamassa, M. Milanesio, C. Barolo, R. D. Costa, *Dalton Trans.* **2016**, *45*, 8984–8993.
[36] N. Kundu, S. M. Towsif Abtab, S. Kundu, A. Endo, S. J. Teat, M. Chaudhury, *Inorg. Chem.* **2012**, *51*, 2652–2661.
[37] A. L. Guckian, M. Doering, M. Ciesielski, O. Walter, J. Hjelm, N. M. O'Boyle, W. Henry, W. R. Browne, J. J. McGarvey, J. G. Vos, *Dalton Trans.* **2004**, 3943–3949.
[38] E. Fresta, G. Volpi, C. Garino, C. Barolo, R. D. Costa, *Polyhedron* **2018**, *140*, 129–137.
[39] G. Attilio Ardizzoia, S. Brenna, S. Durini, B. Therrien, *Organometallics* **2012**, *31*, 5427–5437.
[40] G. Attilio Ardizzoia, S. Brenna, B. Therrien, *Dalton Trans.* **2012**, *41*, 783–790.
[41] G. Attilio Ardizzoia, S. Brenna, B. Therrien, *Eur. J. Inorg. Chem.* **2010**, 3365–3371.
[42] G. Attilio Ardizzoia, S. Brenna, F. Castelli, S. Galli, N. Masciocchi, *Inorg. Chim. Acta* **2010**, *363*, 324–329.
[43] D. Tzimopoulos, S. Brenna, A. Czapik, M. Gdaniec, A. Ardizzoia, P. D. Akrivos, *Inorg. Chim. Acta* **2012**, *383*, 105–111.
[44] G. A. Ardizzoia, S. Brenna, S. Durini, I. Trentin, B. Therrien, *Dalton Trans.* **2013**, *42*, 12265–12273.
[45] G. A. Ardizzoia, S. Brenna, S. Cenini, G. La Monica, N. Masciocchi, A. Maspero, *J. Mol. Catal. A* **2003**, *204–205*, 333–340.
[46] N. Masciocchi, G. A. Ardizzoia, G. La Monica, A. Maspero, S. Galli, A. Sironi, *Inorg. Chem.* **2001**, *40*, 6983–6989.
[47] G. A. Ardizzoia, S. Brenna, *Coord. Chem. Rev.* **2016**, *311*, 53–74.
[48] G. A. Ardizzoia, S. Brenna, F. Castelli, S. Galli, C. Marelli, A. Maspero, *J. Organomet. Chem.* **2008**, *693*, 1870–1876.
[49] G. A. Ardizzoia, S. Brenna, S. Durini, B. Therrien, M. Veronelli, *Eur. J. Inorg. Chem.* **2014**, 4310–4319.
[50] G. A. Ardizzoia, S. Brenna, S. Durini, B. Therrien, *Polyhedron* **2015**, *90*, 214–220.
[51] S. Durini, G. A. Ardizzoia, B. Therrien, S. Brenna, *New J. Chem.* **2017**, *41*, 3006–3014.
[52] G. A. Ardizzoia, D. Ghiotti, B. Therrien, S. Brenna, *Inorg. Chim. Acta* **2018**, *471*, 384–390.
[53] H. Geneste, B. Schäfer, *Synthesis* **2001**, *15*, 2259–2262.
[54] L. Yang, D. R. Powell, R. P. Houser, *Dalton Trans.* **2007**, 955–964.
[55] C. Hansch, A. Leo, R. W. Taft, *Chem. Rev.* **1991**, *91*, 165–195.
[56] D. Mandal, A.-Q. Wu, G.-C. Guo, D. Ray, *Inorg. Chem.* **2006**, *45*, 8826–8828.
[57] G. M. Sheldrick, *Acta Crystallogr., Sect. A* **2008**, *64*, 112–122.
[58] L. J. Farrugia, *J. Appl. Crystallogr.* **1997**, *30*, 565.
[59] a) G. te Velde, F. M. Bickelhaupt, E. J. Baerends, C. Fonseca Guerra, S. J. A. van Gisbergen, J. G. Snijders, T. Ziegler, *J. Comput. Chem.* **2001**, *22*, 931–967; b) C. Fonseca Guerra, J. G. Snijders, G. te Velde, E. J. Baerends, *Theor. Chem. Acc.* **1998**, *99*, 391–403; c) E. J. Baerends, T. Ziegler, J. Autschbach, D. Bashford, A. Bérces, F. M. Bickelhaupt, C. Bo, P. M. Boerrigter, L. Cavallo, D. P. Chong, L. Deng, R. M. Dickson, D. E. Ellis, M. van Faassen, L. Fan, T. H. Fischer, C. Fonseca Guerra, M. Franchini, A. Ghysels, A. Giammona, S. J. A. van Gisbergen, A. W. Götz, J. A. Groeneveld, O. V. Gritsenko, M. Grüning, S. Gusarov, F. E. Harris, P. van den Hoek, C. R. Jacob, H. Jacobsen, L. Jensen, J. W. Kaminski, G. van Kessel, F. Kootstra, A. Kovalenko, M. V. Krykunov, E. van Lenthe, D. A. McCormack, A. Michalak, M. Mitoraj, S. M. Morton, J. Neugebauer, V. P. Nicu, L. Noodleman, V. P. Osinga, S. Patchkovskii, M. Pavanello, P. H. T. Philipsen, D. Post, C. C. Pye, W. Ravenek, J. I. Rodríguez, P. Ros, P. R. T. Schipper, H. van Schoot, G. Schreckenbach, J. S. Seldenthuis, M. Seth, J. G. Snijders, M. Solà, M. Swart, D. Swerhone, G. te Velde, P. Vernooijs, L. Versluis, L. Visscher, O. Visser, F. Wang, T. A. Wesolowski, E. M. van Wezenbeek, G. Wiesenekker, S. K. Wolff, T. K. Woo, A. L. Yakovlev, ADF2017, SCM, Theoretical Chemistry, Vrije Universiteit, Amsterdam, The Netherlands, http://www.scm.com.
[60] S. Grimme, J. Antony, S. Ehrlich, S. Krieg, *J. Chem. Phys.* **2010**, *132*, 154104.
[61] D. P. Chong, *Mol. Phys.* **2005**, *103*, 749–761.
[62] a) A. Klamt, G. J. Schürmann, *J. Chem. Soc., Perkin Trans. 2* **1993**, 799–805; b) A. Klamt, V. Jonas, *J. Chem. Phys.* **1996**, *105*, 9972–9981; c) C. C. Pye, T. Ziegler, *Theor. Chem. Acc.* **1999**, *101*, 396–408.

Received: January 22, 2019